Thesis/
Reports
White,
G.C.

Research and Development on New Methods for Monitoring Mexican Spotted Owl Populations

RJVA 00-JV11221607-133

CD020711

RMRS LIBRARY - OGDEN CENTER
MONTHLY ALERT
Edition JUL 2002
Item No. 266
Title RMF

PROVIDED BY
THE RMRS LIBRARY
MATERIAL MAY BE PROTECTED BY
COPYRIGHT LAW, TITLE 17 US CODE

RESEARCH AND DEVELOPMENT ON NEW METHODS FOR MONITORING MEXICAN SPOTTED OWL POPULATIONS

Final Report
Submitted to Rocky Mountain Research Station
RJVA 00-JV11221607-133

Gary C. White
Department of Fishery and Wildlife Biology
Colorado State University
Fort Collins, CO 80523

Alan B. Franklin
Colorado Cooperative Fish & Wildlife Research Unit
Colorado State University
Fort Collins, CO 80523

David C. Bowden
Department of Statistics
Colorado State University
Fort Collins, CO 80523

15 December 2001

266. White, Gary C. ; Franklin, Alan B. ; Bowden, David C. *Research and development on new methods for monitoring Mexican spotted owl populations.* 2001: 88 p. [Unpublished Final Report to RMRS; RJVA 00-JV11221607-133] 34

EXECUTIVE SUMMARY

Four topics were explored to improve methods for monitoring Mexican Spotted Owl populations. First, an improved population size estimator was obtained using a ratio estimator with the TIN ratio − 1 or the TIN ratio − 1 raised to the 1.52 power as a covariate. The TIN ratio is the ratio of true surface area to the planar area (TIN_Area/Area). Surface area is the true area that lies within each quadrat calculated by deriving TINs (Triangulated Irregular Networks) for each quadrat using USGS Digital Elevation Models. The TIN ratio will always be ≥1, hence, we subtracted 1 from the ratio so that the minimum value is zero, and thus passes through the origin. Ratio estimators of population size with the TIN Ratio as a covariate were more precise than using area. With population estimates from the high density strata quadrats, assuming no sampling variation for these estimates, a CV of 10% for the covariate (TIN Ratio − 1)$^{1.52}$ is obtained, compared to 32% for area. Thus, we conclude that auxiliary covariates based on topographical features can be used to obtain relatively precise estimates of population size. We believe that if habitat covariates were available, even greater reductions in precision would be obtained through use of a multivariate ratio estimator.

Second, we explored the potential effects of reducing quadrat size to 35 - 50 km^2 on 1) the magnitude and sampling variance of density estimates, 2) temporal process variation in density estimates, and 3) incidence of movement across quadrat boundaries by owls holding territories near quadrat boundaries. The 2 demographic study areas were subdivided into *large quadrats* (those of the size used in the pilot study) and *small quadrats* (quadrats approximately half the size of those sampled in 1999). The total number of distinct individuals within a quadrat was considered estimated without error, that is, with no sampling variance. Annual estimates of density were similar between large and small quadrats indicating that density was not inflated due to smaller study area size. Annual rates of territories crossing boundaries in small quadrats was almost identical to rates for large quadrats. Thus, we conclude that reduction in size of the quadrats sampled will not cause biased estimates of owl population size.

Third, because of the temporal variation in population dynamics, we estimated the probability that the Mexican Spotted Owl population in the 3 recovery units to be monitored will decline by 20% over a 10-year period even if the mean population growth rate equals 1. Temporal process variance in the rate of population change, λ, was estimated from the demographic study areas to be $\hat{\sigma}_{\lambda} = 0.114$. With this level of temporal variation, the probability that the population will decline 20% is 31%. Thus, we conclude that the delisting criteria in the Recovery Plan should be changed to detect a decline of 40%, likely in only 1 10-year interval out of 10.

Finally, we were not successful in modifying existing analytical procedures to estimate the power of the monitoring plan if non-zero process variance is assumed. Monte Carlo simulations are required to correctly estimate power. With a sampling CV of 10% and a range of process standard deviations, we found that power to detect a decline that occurs 1 realization out of 10 is ≤80%. For a fixed sampling CV, power increases to detect declines that occur with a specified probability as process variance increases. However, because we believe that the process standard deviation of $\hat{\sigma}_{\lambda} = 0.114$ may be greater than expected for σ_{λ} for the entire

recovery unit, we conclude that power to detect a 1 in 10 decline with sampling CV of 10% is <80%.

INTRODUCTION

This report consists of 4 parts: evaluation of available covariates to use in a ratio estimator to estimate population size, evaluation of reducing quadrat size to estimate the owl populations, evaluation of the impact of process variation of λ (population rate of change) on the probability that the Mexican Spotted Owl population in the 3 recovery units to be monitored will decline by ≥20% over a 10-year period even if the mean population growth rate equals 1, and evaluation of the impact of process variation of λ (σ^2_λ) on the power of a test to detect trends in the population.

EVALUATION OF COVARIATES TO ESTIMATE POPULATION SIZE

Several changes have been made to the procedures described by Ganey et al. (2000) in their report on estimation of population size based on the pilot study data.

1) Ratio estimators were computed using quadrat area and TIN Ratio - 1. In the following equations, quadrat area is used to illustrate the estimator. We then used these equations to examine an alternative covariate, TIN Ratio - 1, that we used instead of quadrat area. The TIN ratio is the true surface area to the planar area (TIN area ÷ planar area) for each quadrat. Surface area is the true area that lies within each quadrat calculated by deriving TINs (Triangulated Irregular Networks) for each quadrat using USGS Digital Elevation Models This ratio will always be ≥1, hence, we subtracted 1 from the ratio so that the minimum value is zero, and hence passes through the origin. TIN Ratio - 1 was used as a covariate in the ratio estimator because a correlation of 0.847 was found between this variable and $\hat{N}_{hq}$ for the combined strata (0.923 for High strata, 0.379 for Low strata). These correlations are much better than the correlation with quadrat area, which were 0.381 for the combined strata (0.389 for High strata, -0.138 for Low strata).

2) The estimator of the variance of ratio estimator formula was changed. This slight modification of the estimator is more efficient than the original version when the ratio $\frac{A_h}{\bar{a}_h}$ differs from U_h.

3) The number of quadrats in each strata and the area of quadrats in the sample were revised to reflect the values obtained from the database provided by USFS in October, 2000.

Estimating Total Population Size on the Recovery Unit

To compute the total population size for the recovery unit ($\hat{N}_{RU}$), a ratio estimator was used following Cochran (1977) where the ratio of estimated population size for the sampled quadrats (sum of $\hat{N}_{hq}$ obtained from the $\hat{\boldsymbol{N}}_{\boldsymbol{quadrat}}$ vector, where h is the strata and q is the quadrat) to area of the sampled quadrats (sum of a_{hq}) is multiplied by the stratum area (with A_h the area of each strata h) :

$$\hat{N}_{RU} = \sum_{h=1}^{2} \hat{N}_h' = \sum_{h=1}^{2} \hat{R}_h A_h$$

where

$$\hat{R}_h = \frac{\sum_{q=1}^{u_h} \hat{N}_{hq}}{\sum_{q=1}^{u_h} a_{hq}}$$

In our case, we have only two strata (low or high density). Because sampled quadrat population sizes are estimates instead of exact counts, and because of the covariances of the $\hat{N}_{hq}$ induced by estimating common resighting probabilities across quadrats and strata, the estimated variance of $\hat{N}_{RU}$ [$\hat{\text{V}}\text{ar}(\hat{N}_{RU})$] is considerably more complicated than the usual case:

$$\hat{\text{V}}\text{ar}(\hat{N}_{RU}) = \sum_{h=1}^{2} \left(\frac{A_h}{\bar{a}_h}\right)^2 \left(\frac{1}{u_h} - \frac{1}{U_h}\right) \sum_{q=1}^{u_h} \frac{\left(\hat{N}_{hq} - \hat{R}_h a_{hq}\right)^2}{u_h - 1}$$

$$+ \sum_{h=1}^{2} \frac{\left(\frac{A_h}{\bar{a}_h}\right)^2}{u_h} \left[\sum_{q=1}^{u_h} \frac{\hat{\text{V}}\text{ar}(\hat{N}_{hq})}{u_h} + \sum_{q=1}^{u_h} \sum_{q' \neq q}^{u_h} \frac{\hat{\text{c}}\text{ov}(\hat{N}_{hq}, \hat{N}_{hq'})}{u_h}\right]$$

$$+ \sum_{h=1}^{2} \sum_{h \neq h'}^{2} \frac{\left(\frac{A_h}{\bar{a}_h}\right)\left(\frac{A_{h'}}{\bar{a}_{h'}}\right)}{u_h u_{h'}} \sum_{q=1}^{u_h} \sum_{q'=1}^{u_{h'}} \hat{\text{c}}\text{ov}(\hat{N}_{hq}, \hat{N}_{h'q'})$$

$$- \sum_{h=1}^{2} \left(\frac{A_h}{\bar{a}_h}\right)^2 \left(\frac{1}{u_h} - \frac{1}{U_h}\right) \left[\sum_{q=1}^{u_h} \frac{\hat{\text{V}}\text{ar}(\hat{N}_{hq})}{u_h} - \sum_{q=1}^{u_h} \sum_{q' \neq q}^{u_h} \frac{\hat{\text{c}}\text{ov}(\hat{N}_{hq}), \hat{N}_{hq'})}{u_h(u_h - 1)}\right],$$

where $\bar{a}_h$ is the average area of quadrats in the sample. The first term of this equation is the variation in the $\hat{N}_{hq}$ multiplied by a finite correction factor. The second term incorporates the sampling variation within quadrats while the third term incorporates the covariances between quadrats. The final term is a correction term that subtracts out mean sampling variance and covariances adjusted by a finite population correction factor. Finite population correction factors are incorporated into the equation because we sampled from a finite sampling frame. A

reasonable approximation to this equation where the finite population correction is ignored and $u_h^2 \approx u_h(u_h - 1)$is:

$$\hat{\text{Var}}(\hat{N}_{RU}) = \sum_{h=1}^{2} \frac{\left(\frac{A_h}{\bar{a}_h}\right)^2}{u_h}\left[\sum_{q=1}^{u_h} \frac{\left(\hat{N}_{hq} - \hat{R}_h a_{hq}\right)^2}{u_h - 1}\right]$$

$$+ \sum_{h=1}^{2} \frac{\left(\frac{A_h}{\bar{a}_h}\right)^2}{u_h(u_h - 1)} \sum_{q=1}^{u_h} \sum_{q' \neq q}^{u_h} \hat{\text{cov}}(\hat{N}_{hq}, \hat{N}_{hq'})$$

$$+ \sum_{h \neq h'} \frac{\left(\frac{A_h}{\bar{a}_h}\right)\left(\frac{A_{h'}}{\bar{a}_{h'}}\right)}{u_h u_{h'}} \sum_{q=1}^{u_h} \sum_{q'=1}^{u_{h'}} \hat{\text{cov}}(\hat{N}_{hq}, \hat{N}_{h'q'}) \quad .$$

In this equation, the first term is the variation in the $\hat{N}_{hq}$, the second term incorporates the covariances within strata, and the third term incorporates the covariances across strata. These equations are extensions of the formulae given by Skalski (1994) because they incorporate the covariances of the $\hat{N}_{hq}$ across quadrats and strata.

Alternative Covariates to Quadrat Area

With the ratio estimator based on area of quadrat, the estimate of population size, using $\hat{N}_q$, for the recovery unit [$\hat{N}_{RU}$ = 2940.6, $\hat{\text{SE}}(\hat{N}_{RU})$ = 1075.4] had a coefficient of variation (CV) of 37% (Table 1). If the sampling variance of $\hat{N}_q$ is ignored (Table 1), the CV is reduced to 32%. The lowest achievable CV based on quadrat area is 27% where just the raw counts of owls (M_{t+1}) are used in the ratio estimator of $\hat{N}_q$ with no adjustment of these counts by p^*, the owl detection probability.

The variable TIN Ratio - 1 has a strong correlation with quadrat estimated population size $\hat{N}_q$ (Figure 1). With the ratio estimator based on TIN Ratio - 1, the estimate of population size for the recovery unit [$\hat{N}_{RU}$ = 2172.8, $\hat{\text{SE}}(\hat{N}_{RU})$ = 519.6] had a coefficient of variation (CV) equal to 24% (Table 2). If the sampling variance of $\hat{N}_q$ is ignored (Table 2), the CV is reduced to 16%. Again, the lowest achievable CV based on using TIN Ratio - 1 is 14% where just the raw counts of owls (M_{t+1}) are used in the ratio estimator of $\hat{N}_q$ with no adjustment of these counts by p^*.

Table 1. Results of estimating the density and population size for the low and high density strata in the Upper Gila Recovery Unit (not including tribal lands) with quadrat area as the ratio covariate.

Population Estimate	Strata	Strata Population ($\hat{N}$)	$\widehat{SE}(\hat{N})$	CV
$\hat{N}_q$	High	2896.6	1073.6	37.1%
	Low	44.0	44.2	100.5%
	Recovery Unit	2940.6	1075.4	36.6%
$\hat{N}_q$ without Var($\hat{N}_q$)	High	2896.6	936.0	32.3%
	Low	44.0	44.2	100.5%
	Recovery Unit	2940.6	937.0	31.9%
M_{t+1}	High	2084.1	578.4	27.8%
	Low	39.5	39.8	100.8%
	Recovery Unit	2123.7	579.7	27.3%

Table 2. Results of estimating the density and population size for the low and high density strata in the Upper Gila Recovery Unit (not including tribal lands) with TIN Ratio -1 as the ratio covariate.

Population Estimate	Strata	Strata Population ($\hat{N}$)	$\widehat{SE}(\hat{N})$	CV
$\hat{N}_q$	High	2144.9	518.1	24.2%
	Low	27.9	25.7	92.1%
	Recovery Unit	2172.8	519.6	23.9%
$\hat{N}_q$ without Var($\hat{N}_q$)	High	2144.9	341.9	15.9%
	Low	27.9	25.7	92.1%
	Recovery Unit	2172.8	342.8	15.8%
M_{t+1}	High	1543.3	220.6	14.3%
	Low	25.1	23.1	92.0%
	Recovery Unit	1568.4	221.8	14.1%

We explored alternate relationships to the simple linear relationship between TIN ratio-1 and $\hat{N}_q$ discussed previously. The variable TIN Ratio - 1 raised to the 1.52 power also had a very strong correlation with $\hat{N}_q$ (Figure 2). With the ratio estimator based on TIN Ratio - 1 raised to the 1.52 power, the estimate of population size for the recovery unit [$\hat{N}_{RU}$ = 1976.4, $\widehat{SE}(\hat{N}_{RU})$ = 408.8] had a coefficient of variation (CV) of 21% (Table 3). If the sampling variance of $\hat{N}_q$ is ignored (Table 3), the CV is reduced to 10%, the lowest achievable CV. The CV is 15% when just the raw counts of owls (M_{t+1}) are used in the ratio estimator of $\hat{N}_q$ with no adjustment of these counts by p^*.

Table 3. Results of estimating the density and population size for the low and high density strata in the Upper Gila Recovery Unit (not including tribal lands) with TIN Ratio - 1 raised to the 1.52 power as the ratio covariate.

Population Estimate	Strata	Strata Population ($\hat{N}$)	$\widehat{SE}(\hat{N})$	CV
$\hat{N}_q$	High	1949.7	407.1	20.9%
	Low	26.7	24.4	91.4%
	Recovery Unit	1976.4	408.8	20.7%
$\hat{N}_q$ without Var($\hat{N}_q$)	High	1949.7	201.2	10.3%
	Low	26.7	24.4	91.4%
	Recovery Unit	1976.4	202.6	10.3%
M_{t+1}	High	1402.8	218.0	15.5%
	Low	24.0	21.9	91.3%
	Recovery Unit	1426.8	219.1	15.4%

POTENTIAL EFFECTS OF QUADRAT SIZE ON MEXICAN SPOTTED OWL DENSITY ESTIMATES

The objectives of this analysis were to explore the potential effects of reducing quadrat size to 35 - 50 km^2 on 1) the magnitude and sampling variance of density estimates, 2) temporal process variation in density estimates, and 3) incidence of movement across quadrat boundaries by owls holding territories near quadrat boundaries. Density was used as the basis for comparison to remove the effects of differing quadrat areas.

Comparisons were made between quadrats of the size used in the pilot study conducted in 1999 and quadrats approximately half the size of those sampled. Two study areas delineated to investigate the demography of Mexican Spotted owls were used to develop these comparisons (Seamans et al. 1999). One study area, located in Arizona, was 584.4 km^2 while the other, located in New Mexico, was 453.1 km^2. Mexican spotted owls have been color-marked and resighted annually on each study area from 1991 through 1999. Personnel conducting these studies provided data on spotted owl locations (roost and nest sites occupied by pairs, single males or single females) with one location representing a unique spotted owl territory for each year. Territory locations were delineated based on color-marked birds and geographic locations. These data provided the basis for estimating density within quadrats. The study areas were subdivided into *large quadrats* (those of the size used in the pilot study) and *small quadrats* (those approximately half the size of those sampled in 1999) using the following approach:

1) determining the appropriate size of large and small quadrats by examining the sampling frame and quadrats actually sampled in 1999 during the monitoring pilot study;

2) partitioning the demography study areas into large and small quadrats prior to viewing the spotted owl location data;

3) estimating density within large and small quadrats;

4) comparing annual densities and temporal process variation estimated from large quadrats with estimates from small quadrats; and

5) examining the degree to which territories crossed quadrat boundaries and whether small quadrats had a greater incidence than large quadrats.

The first step in determining quadrat size was to examine the distributions of the 744 quadrats in the sampling frame delineated by the Upper Gila Recovery Unit and the 25 quadrats sampled during the Mexican Spotted Owl Monitoring Pilot Study (Figure 3). Mean quadrat size was 61.06 km^2 for the entire sampling frame (median = 59.55, SD = 17.61, range = 25.00, 99.28 km^2) and 61.96 km^2 for the quadrats sampled in 1999 (median = 62.44, SD = 8.02, range = 43.68, 76.40 km^2). Sampled quadrats were concentrated around the mid-range of the available quadrats in the sampling frame. The decision was made to use quadrat sizes between 45 and 80 km^2 in delineating large quadrats on the study areas to encompass the range of the sampled quadrats and to capture 78% of the quadrat sizes in the sampling frame. An attempt was made to maintain quadrat sizes of around 50 to 60 km^2 where feasible. Small quadrats were then delineated as one-half of the large quadrats except where sizes of small quadrats would be less than 20 km^2. In those case, large quadrats were left intact and included with the remaining small quadrats.

GIS coverages of each study area were supplied that included entire watersheds and portions of watershed clipped by the study area boundary that represented quadrats from the original sampling frame (Figure 4A). Topographic features underlying each study area were incorporated as a separate GIS layer by edge-matching 1:24000 U. S. Geological Survey topographic maps (supplied as graphics files). Edge-matching provided seamless topographic coverage underlying each study areas. Large quadrats were on each study area were delineated in two ways (Figure 4A and 4B). First, existing watersheds on each study area were combined into larger quadrats. This was done where smaller portions of original watersheds had been clipped by the study area boundary. Second, these new quadrat boundaries were manually adjusted in ArcView® GIS (version 3.2) by placing the new quadrat boundaries over the topographic layer and then manually moving boundary line vertices onto ridges and other prominent topographic features. This was done because the watershed boundaries were originally delineated using coarser resolutions. Once large quadrat boundaries had been established on each study area, small quadrats boundaries were developed by splitting large quadrats into small quadrats with the constraint that small quadrats could not be less than 20 km^2 (Figure 4C). Small quadrat boundaries were drawn and incorporated as polygons using the Split Quadrat feature in ArcView. Boundaries were manually drawn using underlying topographic features and followed ridges and major topographic features as closely as possible. All large and small quadrats were developed prior to viewing the locations of spotted owls within the study areas to avoid biases in delineating quadrat boundaries.

Once quadrat boundaries had been established, a GIS coverage of owl locations was developed. A data file containing owl locations within each quadrat was developed by using the Spatial Join feature in ArcView using the owl location and quadrat boundary coverages. This

was done separately for large and small quadrats. Empty quadrats were added to this data file because the spatial join operation only included quadrats containing owl locations. This data file was used as input to SAS code written to estimate annual estimates of density separately for large and small quadrats where 1) the number of individuals were computed for each quadrat for each year (including those quadrats containing no owls), 2) the density of each quadrat was estimated using the number of individuals and size of the quadrat (in km^2), and 3) mean density, it's standard deviation and standard error was estimated for each year.

In this analysis, the total number of distinct individuals within a quadrat was considered estimated without error, that is, with no sampling variance. These estimates were analogous to M_{t+1} in the power analyses of N in the monitoring pilot study. Therefore, the arithmetic standard deviation associated with mean annual densities was considered an estimate of the spatial process standard deviation ($\sigma_{spatial}$) among quadrats within each year. Annual estimates of $\sigma_{spatial}$ were expressed as coefficients of spatial process variation ($CV_{spatial}$):

$$\frac{\sigma_{spatial}}{\bar{\hat{D}}}.$$

Temporal process variation was estimated only for small quadrats because the interest was centered around whether small quadrats could be appropriately used. Because the mean annual estimates had sampling variance associated with them ($\widehat{var}(\hat{D}) = [\widehat{se}(\hat{D})]^2$), we used a method-of-moments random-effects model utilizing shrinkage estimators to estimate $\sigma^2_{temporal}$, $\bar{D}$, and $se(\bar{D})$, using an intercepts-only model, and β_1 (trend in estimates over time) and $\sigma_{residual}$, using a linear trend model. These models accounted for (and removed) the sampling variation from the total variation to estimate temporal process variation. In the linear trend models, $\sigma_{residual}$ was the amount of temporal process variation remaining after a linear trend had been accounted for. This analysis was done with the estimates for all nine years and for only the last seven years (with the first two years removed). The latter analysis reflected the potential for a "learning" effect where numbers of owls may have been underestimated because the investigators were still learning the extent of the study areas.

The degree to which territories crossed quadrat boundaries in different years was evaluated in three ways for large and small quadrats separately. First, the number of territories crossing boundaries in different years (e.g., a territory found in one quadrat in one year being found in another quadrat in a different year) was computed across all the years. This was simple enumeration of the number territories crossing quadrat boundaries. Second, we estimated annual rates of territories crossing boundaries by dividing the number of territories in year t+1 that were on quadrats different from those in the year t divided by the total number of territories in year t that were available for re-observation in year t+1. The denominator did not include territories that were observed in one year but not the next.

Distributional properties of quadrats from demography areas

A total of 18 large and 35 small quadrats were delineated on the two study areas. Sizes of large quadrats were somewhat smaller than those sampled during the monitoring pilot study (Figure 5). However, the large quadrats had distributional properties more similar to the

sampling frame than to the quadrats sampled during the monitoring pilot study (Table 4). The distributional properties of the small quadrats was about half that of the large quadrats (Table 4).

Table 4. Distributional properties of quadrat sizes from sampling frame, sampled quadrats used in monitoring pilot study, and large and small quadrats delineated on demography study areas.

	Quadrat size (km^2)			
Statistic	Sampling Frame	Pilot Study Sample	Large Quadrats from Study Areas	Small Quadrats from Study Areas
Mean	61.06	61.96	57.65	29.65
Median	59.55	62.44	54.57	27.97
SD	17.61	8.02	14.44	5.79
Minimum	25.00	43.68	39.45	22.42
Maximum	99.28	76.40	86.61	44.23
n	744	25	18	35

Comparison of density estimates between large and small quadrats

Annual estimates of density were similar between large and small quadrats (Figure 6) indicating that density was not inflated due to smaller study area size. In addition, density estimates from the large and small quadrats were also similar to annual density estimates averaged across the two study areas (Figure 6). Based on averages across years for each set of quadrats, the ratio of mean standard errors for the density estimates from small:large quadrats was 0.875 (0.014/0.016) indicating a 12.5% improvement by using the small quadrats. However, annual estimates of coefficients of spatial process variation were higher for small quadrats (Figure 7) with small quadrats having higher CV's than large quadrats. Based on averages across years for each set of quadrats, the ratio of mean spatial process standard deviations for the density estimates from small:large quadrats was 1.239 (0.083/0.067) indicating a 23.9% increase by using the small quadrats. This increase may be due to the clumped spatial distribution of owls across the landscape.

The estimates of temporal process standard deviation (based on the random effects means models) were high for both the 9-year period and 7-year period, which removed the potentail "learning" effect (Table 5). Coefficients of process variation were 0.251 and 0.296 for the 9-year and 7-year periods, respectively. The amount of temporal process variation was not reduced substantially by the linear model for the 9-year period but was reduced considerably by the linear model for the 7-year period. This suggests that if there is a learning effect and a linear

trend is evident, temporal process variation around the trend line was minimal when the small quadrats were used.

Table 5. Parameter estimates from means and linear trend models of Mexican spotted owl density estimated from small quadrats over 9- and 7-year periods. Estimates of σ^2 from the means model represent temporal process variation while estimates from the linear trend model represent residual temporal variation remaining from that variation accounted for by the model.

	Estimates from means model for:		Estimates from trend model for:	
Parameter	9 years	7 years	9 years	7 years
β_0	0.0894	0.0893	0.1168	0.1369
SE(β_0)	0.0088	0.0113	0.0181	0.0159
β_1	—	—	-0.0054	-0.0120
SE(β_1)	—	—	0.0032	0.0034
σ^2	0.0005	0.0007	0.0004	0.0001
	(0.0002, 0.0034)	(0.0001, 0.0030)	(0.0001, 0.0023)	(0.0000, 0.0006)
σ	0.0224	0.0265	0.0200	0.0100

Rates of territories crossing quadrat boundaries

Annual rates of territories crossing boundaries in small quadrats was almost identical to rates for large quadrats (Table 6). In only two years (1997 and 1998) did the rates differ slightly. This difference was due to two territories crossing small quadrat boundaries (see Table 6). There appeared to be an increase in rates of territories crossing quadrat boundaries over time. This may be due to a general shifting in territories over time.

Table 6. Annual rates of territories crossing boundaries for large and small quadrats delineated from demography study areas.

Year	No. territories in year *t*	No. territories found in different quadrat in year *t*+1		Rate of territories crossing boundaries	
		Large quadrats	Small quadrats	Large quadrats	Small quadrats
1991	42				
1992	57	1	1	0.024	0.024
1993	62	1	1	0.018	0.018
1994	51	2	2	0.032	0.032
1995	44	1	1	0.020	0.020
1996	32	7	7	0.159	0.159
1997	32	4	5	0.125	0.156
1998	29	2	3	0.063	0.094
1999	—	5	5	0.172	0.172

ESTIMATION OF THE PROBABILITY OF A 20% DECLINE

Because of process variation, the Mexican Spotted Owl population could decline 20% just by chance, even though the mean population rate of increase is 0 ($\lambda = 1$). To determine the probability of such a scenario, we estimated the process variance of λ (σ^2_λ) from the encounter history data on the demographic study areas in Arizona and New Mexico. These areas were surveyed each year from 1991 to 1999. Two approaches to estimating σ^2_λ were used.

First, the number of owls observed on both of the study areas for each year was determined, and the corresponding annual estimate of λ computed as the ratio of consecutive counts, i.e., $\lambda = N_{t+1}/N_t$, where N_t is the combined number of owls observed on both study areas in year t. The first 2 estimates of λ for the intervals 1991-2 and 1992-3 were discarded because of difficulties in obtaining nearly complete counts during the first years of both studies, leaving 6 estimates of λ for the combined study areas. The standard deviation of these 6 estimates was SD = 0.175 ($\bar{\lambda} = 0.925$), and this estimate represents the process standard deviation of the population growth rate ($\sigma_\lambda = \sqrt{\sigma^2_\lambda}$) assuming that censuses are accomplished each year. We expect this estimate to be biased high because the 7 counts used to estimate the 6 values of λ likely contain some sampling variation.

The second approach to estimating σ_λ was obtained with estimates of λ from the Pradel (1996) model in Program MARK (White and Burnham 1999). The 5 estimates of λ from the model $\{\phi(t), p(\text{area}*t), \lambda(t)\}$ for the 2 study areas were used to estimate σ_λ. The first 2 estimates were discarded because of suspected changes in the size and composition of the study areas, and the value of λ for the first and last intervals is not estimable with the model $\{\phi(t),$

p(area*t), $\lambda(t)$}. From the variance components estimator of Program MARK (White et al. 2001), the process standard deviation for these 5 estimates was $\hat{\sigma}_{\lambda} = 0.114$, with 95% confidence interval of 0.040 to 0.377. Mean λ was 0.905 with SE 0.0557. We expect this estimate of σ_{λ} to be less biased than the previous value obtained from consecutive counts because the λ estimates have been corrected for owl detection probabilities.

Each of these estimates were used to simulate 1,000,000 values of the product $\prod_{i=1}^{9} \lambda_i$, where λ_i was drawn from a normal distribution with mean 1 and standard deviation equal to the appropriate estimate of σ_{λ}. The proportion of the simulations with the product less than 0.9, 0.8, and 0.5 represent the probability of the owl population declining 10%, 20%, and 50%, respectively. Results are shown in Table 7.

Table 7. Probability of the Mexican Spotted Owl population declining by 10%, 20%, or 50% assuming that the population rate of growth is distributed with process standard deviation of 0.175 or 0.114, and mean $\lambda = 1$. Both a normal and beta distribution were simulated. These probabilities are based on 1,000,000 simulations, so standard errors of the estimates are $\sqrt{\hat{p}(1 - \hat{p})/1{,}000{,}000}$.

Distribution	Bounds	Decline	Probability of a decline where:	
			$\sigma_{\lambda} = 0.175$	$\sigma_{\lambda} = 0.114$
Normal	$-\infty$, ∞	10%	0.515	0.439
		20%	0.429	0.312
		50%	0.156	0.037
Beta	0.6, 1.487	10%	0.521	0.441
		20%	0.434	0.312
		50%	0.151	0.033
Beta	0.75, 1.487	10%	0.527	0.446
		20%	0.436	0.313
		50%	0.138	0.027

To assess the sensitivity of the results in Table 7 to the assumption of a normal distribution, 2 beta distributions were also examined. To set the upper bound on the distribution of λ, a projection matrix was developed:

$$L = \begin{bmatrix} 0 & s_{SA} f R & s_A f R \\ s_J & 0 & 0 \\ 0 & s_{SA} & s_A \end{bmatrix} ,$$

where s_A = adult survival, s_{SA} = subadult survival, s_J = juvenile survival, f = fecundity, and R = proportion of young that are female. To estimate an upper bound on λ, we assumed the very liberal numerical values of $s_A = 0.95$, $s_{SA} = 0.95$, $s_J = 0.6$, $f = 2.8$, and $R = 0.5$. We obtained an asymptotic value of $\lambda = 1.486744$ based on the dominant eigenvalue of the matrix:

$$\lambda = \frac{s_A + \sqrt{s_A^2 + 4 R s_J s_{SA} f}}{2} .$$

To estimate a lower bound on λ, we assumed the very conservative numerical values of $s_A = 0.6$, $s_{SA} = 0.60$, $s_J = 0.0$, $f = 0.0$, and $R = 0.5$, giving an asymptotic value of $\lambda = 0.60$. As can be seen from the eigenvalue equation, for $f = 0$, the value of λ is always just s_A. The value $s_A = 0.6$ was taken from Franklin et al. (2000) for northern spotted owls. A lower bound on λ of 0.75 was also considered.

Values of λ with mean $\bar{\lambda}$ standard deviation $SD(\lambda)$ were simulated from a beta distribution as $B(\alpha, \beta)(\lambda_{upper} - \lambda_{lower}) + \lambda_{lower}$, where $B(\alpha, \beta)$ had a mean of $\mu = \frac{\bar{\lambda} - \lambda_{lower}}{\lambda_{upper} - \lambda_{lower}}$ and standard deviation of $\sigma = \frac{SD(\lambda)}{\lambda_{upper} - \lambda_{lower}}$, giving $\alpha = \frac{-\mu(\mu^2 - \mu + \sigma^2)}{\sigma^2}$, and $\beta = \frac{(\mu - 1)(\mu^2 - \mu + \sigma^2)}{\sigma^2}$.

To verify that the results in Table 7 are approximately correct, we derived analytical results that provide approximate estimates. First, the expected value of of the product $\prod_{i=1}^{9} \lambda_i$ is 1, which is what we found in the simulations. Further, the approximate variance of this product based on a Taylor series expansion (delta method) is

$$\mathrm{var}\left(\prod_{i=1}^{9} \lambda_i \right) = \prod_{i=1}^{9} \lambda_i \sum_{i=1}^{9} CV(\lambda_i)^2 = 9\sigma_\lambda^2 ,$$

although we know that this estimate is biased low. Again, simulation results were verified to be consistent with this analytical result.

The results in Table 7 demonstrate that the delisting criteria in the Mexican Spotted Owl Recovery Plan are unrealistic in that the likelihood of a 20% decline is high for the process variances found from the data collected on the demographic study areas.

The delisting criteria could be set to detect a decline likely at a specified level. The percent decline as a function of various probability levels is shown in Table 8 for the three distributions simulated and the 2 estimates of the process standard deviation.

Table 8. The percent decline expected in the Mexican Spotted Owl population for various probability levels.

Distribution	Bounds	Probability level	Process SD	
			$\sigma_\lambda = 0.175$	$\sigma_\lambda = 0.114$
Normal	$-\infty, \infty$	1 in 4	39.4%	25.1%
		1 in 10	57.4%	39.8%
		1 in 20	65.7%	47.3%
Beta	0.6, 1.487	1 in 4	39.3%	25.1%
		1 in 10	56.4%	39.4%
		1 in 20	64.3%	46.7%
Beta	0.75, 1.487	1 in 4	38.5%	25.0%
		1 in 10	54.5%	38.7%
		1 in 20	61.8%	45.5%

Based on the results in Tables 7 and 8, the selection of the particular distribution, or the lower bound on the Beta distribution, has little effect on the predictions. However, the predictions are extremely sensitive to the process standard deviation. Thus, one of the biggest uncertainties to determining a reasonable decline to monitor for in the Mexican Spotted Owl population in the 3 recovery units is the magnitude of the process standard deviation. We expect that the values obtained from the demographic study areas may be greater than for the population in the 3 recovery units to be monitored because the more extensive area of the 3 recovery units will reduce the effects of localized temporal variation, but we have no other information available from which to estimate σ_λ at this time.

ESTIMATION OF POWER TO DETECT A DECLINE

Results in the previous section demonstrate that detection of a 20% decline in the Mexican Spotted Owl population is not a reasonable goal for the monitoring system. Rather, we conclude that the percent decline of the population that triggers a management action should be based on the probability of observing the decline given the process variance of λ. Because the only estimate of the process standard deviation of λ is based on 2 demographic study areas, we suspect that this estimate may be larger than the process standard deviation for the owl population in the entire recovery unit. Therefore, considerable uncertainty exists concerning the exact value of the process standard deviation of λ to use to design the monitoring program. In this section, we consider how the process standard deviation affects the power to detect trends in

the population, and recommend a monitoring strategy to accommodate uncertainty in our estimates of process variance.

Previous research to evaluate the power of a monitoring program to detect a trend has not considered process variance of λ directly. Gerrodettte (1987) developed analytical formulae for determining power, but assumed that process variance was zero. Hatfield et al. (1996) considered serial correlation of population estimates, but did not consider process variance explicitly. Gibbs (1999, 2000) also has not considered process variance explicitly. For example, although his program MONITOR to simulate power of a monitoring program "can accommodate random trend variation among plots or sites if estimates of its magnitude are available" (Gibbs 2000:228), he assumes "deterministic linear trends are projected from the initial abundance index on each plot over the series of survey years" (Gibbs 2000:225) for analyses presented. He makes no attempt to separate the 2 sources in the estimated CV's presented in the paper with the intent to help readers design population monitoring programs. Thompson et al. (1998) recognized that temporal process variation dictates the level of decline to monitor for, but did not directly incorporate process variation into monitoring programs. They suggested that the analytical results presented by Gerrodette (1987) could be used with non-zero process variance by adding the process variance to the sampling variance to obtain power.

To evaluate the usefulness of Gerrodette's (1987) formulae when process variance is added to the sampling variance as recommended by Thompson et al. (1998), we compared the power estimates obtained from the formulae with power estimates from Monte Carlo simulations. Ten years of population estimates were considered, with a process standard deviation for λ of $\hat{\sigma}_{\lambda} = 0.1135251$, obtained from the Pradel model λ estimates from the 2 demographic study areas. Seven values of the sampling coefficient of variation ($\mathbf{CV}_1$) were considered: 0 to 30% in increments of 5%. Sampling coefficient of variation was assumed constant for population size, and the exponential model of decline, $\hat{N}_i = \hat{N}_1 \lambda^{i-1}$, $i = 1, ..., 10$, was used to detect trend. Taking the natural logarithm of both sides of this equation, we see that $\ln(\hat{N}_i) = \ln(\hat{N}_1) + \ln(\lambda)(i-1)$, so that a linear regression, $y = a + bx$, results, with $\hat{N}_1 = \exp(\hat{a})$ and $\hat{\lambda} = \exp(\hat{b})$. Also, $\mathrm{SE}(\hat{N}_1) \cong \exp(\hat{a})\,\mathrm{SE}(\hat{a})$ and $\mathrm{SE}(\hat{\lambda}) \cong \exp(\hat{b})\,\mathrm{SE}(\hat{b})$. For the Monte Carlo simulations with 10,000 replications, $N_i = N_{i-1}\lambda_{i-1}$, where λ_{i-1} is generated as a random normal deviate with mean 1 and standard deviation 0.1135251. Then, $\hat{N}_i = N_i + \epsilon_i$, where ϵ_i is generated as a random normal deviate with mean zero and standard deviation $\mathbf{CV}_1 N_i$.

Results for $\alpha = 0.05$ (Figures 8, 9) suggest that the analytical approach is invalid because power estimates do not compare favorably with the Monte Carlo simulation results. Most notably, the simulation results demonstrate that the Type I error rate of the trend analysis is not 0.05 as predicted by the analytical procedure. Rather, as would be expected for non-zero process variance and as documented in the previous section, we expect that negative trends in the population trace will occur even when the mean value of λ is one. Further, the power estimates determined via simulation are considerably below estimates from the analytical procedure. Thus, we conclude that simulation procedures are required to determine power for monitoring populations with non-zero process standard deviation.

We also evaluated the bias of estimates of N_1 and λ from the simulations. Percent

relative bias was estimated as

$$\hat{PRB}(\theta) = \frac{\hat{E}(\hat{\theta}) - \theta}{\theta}.$$

A response surface model was fit for both $\hat{\lambda}$ and $\hat{N}_1$ with independent variables of process standard deviation (σ_λ), decline, decline squared, sampling CV and sampling CV squared. AIC model selection was used to select the best model for each variable:

$$\hat{PRB}(\hat{\lambda}) = 0.0528 - 10.404\ \sigma_\lambda + 0.00008182\ CV^2 - 0.00003257\ decline^2, \text{ and}$$

$$\hat{PRB}(\hat{N}_1) = -0.47877 + 9.97573\,\sigma_\lambda + 0.00796\ CV - 0.00380\ CV^2 - 0.00002171\ decline^2.$$

For both $\hat{N}_1$ and $\hat{\lambda}$, relative bias was <4% and <1.5%, respectively, suggesting that the regression estimators are useful for evaluating trend over the range of process standard deviations, sampling CV's, and declines considered in the simulation. Graphs of the these response surfaces are shown in Figures 10-11.

The second issue to address is what level of decline is appropriate to monitor for. We suggest that the appropriate level should be based on the probability of its occurrence. Reasonable values would be declines that only occur 1 realization in 5 to be pro-active (i.e., a higher risk of accepting that a population decline has occurred when the dynamics of the population have not changed), 1 in 10, or 1 in 20 to be very conservative (i.e., willing to accept a high risk of no decline when the dynamics of the population may be changing). The level of decline used to trigger management action should also be a function of the cost of taking management action versus the cost of not taking action, a decision theory problem that is beyond the scope of this research. Hence, in the following, we present power as a function of the probability of decline.

Probability of decline plotted with power for a sampling CV of 10% is shown in Figures 12-14 for 3 levels of process standard deviation: 0.05, 0.1, and 0.15. With $\sigma_\lambda = 0.05$, the monitor program with a sampling CV of 10% has inadequate power to detect a 1 in 10 probability of decline. With $\sigma_\lambda = 0.1$, the monitoring program with sampling CV of 10% would detect a 1 in 10 decline of 35% with power of 68%. With $\sigma_\lambda = 0.15$, the monitoring program with sampling CV of 10% would detect a 1 in 10 decline of 51% with power of 80%.

Another approach to determining the level of decline to monitor for is to consider the probability that a reduced population level will regain the mean level. To evaluate this probability, 100,000 simulations were conducted for 3 levels of process standard deviation: 0.05, 0.10, and 0.15. Populations were started at some fraction of the mean level ranging from 0.5 to 9.99 (Figure 15). Because of the asymmetrical shape of the distribution of population sizes, there is a smaller probability of regaining the mean level from a low initial starting value than there is of dropping to this lower level from the mean value.

CONCLUSIONS

1. Auxiliary covariates based on topographical features can be used to obtain relatively precise estimates of population size, even with relatively small sample sizes of say 20 quadrats per stratum. We believe that if habitat covariates were available, even greater reductions in precision would be obtained. Given the current variables available, we

believe a monitoring program could achieve a sampling CV of 10% with a sample size of 25 quadrats per recovery unit.

2. Reduction in size of the quadrats sampled will not cause biased estimates of owl population size. Because smaller quadrats are more economical, their use will further reduce the cost of the owl monitoring program.

3. The delisting criteria in the Recovery Plan should be changed to detect a decline of 40% or more, instead of the current 20% decline. We believe the likelihood of observing a 40% decline given that the population is stable is about 10% (i.e., 1 10-year interval out of 10 such intervals), whereas the likelihood of observing a 20% decline given that the population is stable is about 31%, or 1 10-year interval out of 3 such intervals.

4. With a sampling CV of 10%, the power to detect a observed 1 of 10 realizations for a range of process standard deviations is never greater than 80%. Monte Carlo simulations must be used to compute the power of the monitoring program if non-zero process variance is assumed.

LITERATURE CITED

Cochran, W. G. 1977. Sampling Techniques. 3rd Edition. John Wiley & Sons, New York, New York, USA. 428pp.

Franklin, A. B. 2000. Climate, habitat quality, and fitness in northern spotted owl populations in northwest California. Ecological Monographs ???.

Ganey, J. L., G. C. White, A. B. Franklin, J. P. Ward, Jr., and D. C. Bowden. 2000. A pilot study on monitoring populations of Mexican spotted owls in Arizona and New Mexico: second interim report. USDA Forest Service Rocky Mountain Research Station, Flagstaff, Arizona.

Gerrodette, T. 1987. A power analysis for detecting trends. Ecology 68:1364-1372.

Gibbs, J. P. 1999. Effective monitoring for adaptive wildlife management: lessons from the Galápagos Islands. Journal of Wildlife Management 63:1055-1065.

Gibbs, J. P. 2000. Monitoring populations. Pages 213-252 *in* L. Boitani and T. K. Fuller, editors. Research Techniques in Animal Ecology: Controversies and Consequences. Columbia University Press, New York, New York, USA.

Hatfield, J. S., W. R. Gould IV, B. A. Hoover, M. R. Fuller, and E. L. Lindquist. 1996. Detecting trends in raptor counts: power and Type I error rates of various statistical tests. Wildlife Society Bulletin 24:505-515.

Pradel, R. 1996. Utilization of capture-mark-recapture for the study of recruitment and population growth rate. Biometrics 52:703-709.

Seamans, M. E., R. J. Gutiérrez, C. A. May, and M. Z. Peery. 1999. Demography of two Mexican spotted owl populations. Conservation Biology 13:744-754.

Skalski, J. R. 1994. Estimating wildlife populations based on incomplete area surveys. Wildlife Society Bulletin 22:192-203.

White, G. C., and K. P. Burnham. 1999. Program MARK: survival estimation from populations of marked animals. Bird Study 46 Supplement:120-138.

White, G. C., K. P. Burnham, and D. R. Anderson. 2001. Advanced features of Program Mark. In press *in* R. Fields, editor. Integrating people and wildlife for a sustainable future. Proceedings of the Second International Wildlife Management Congress. The Wildlife Society, Bethesda, Maryland, USA.

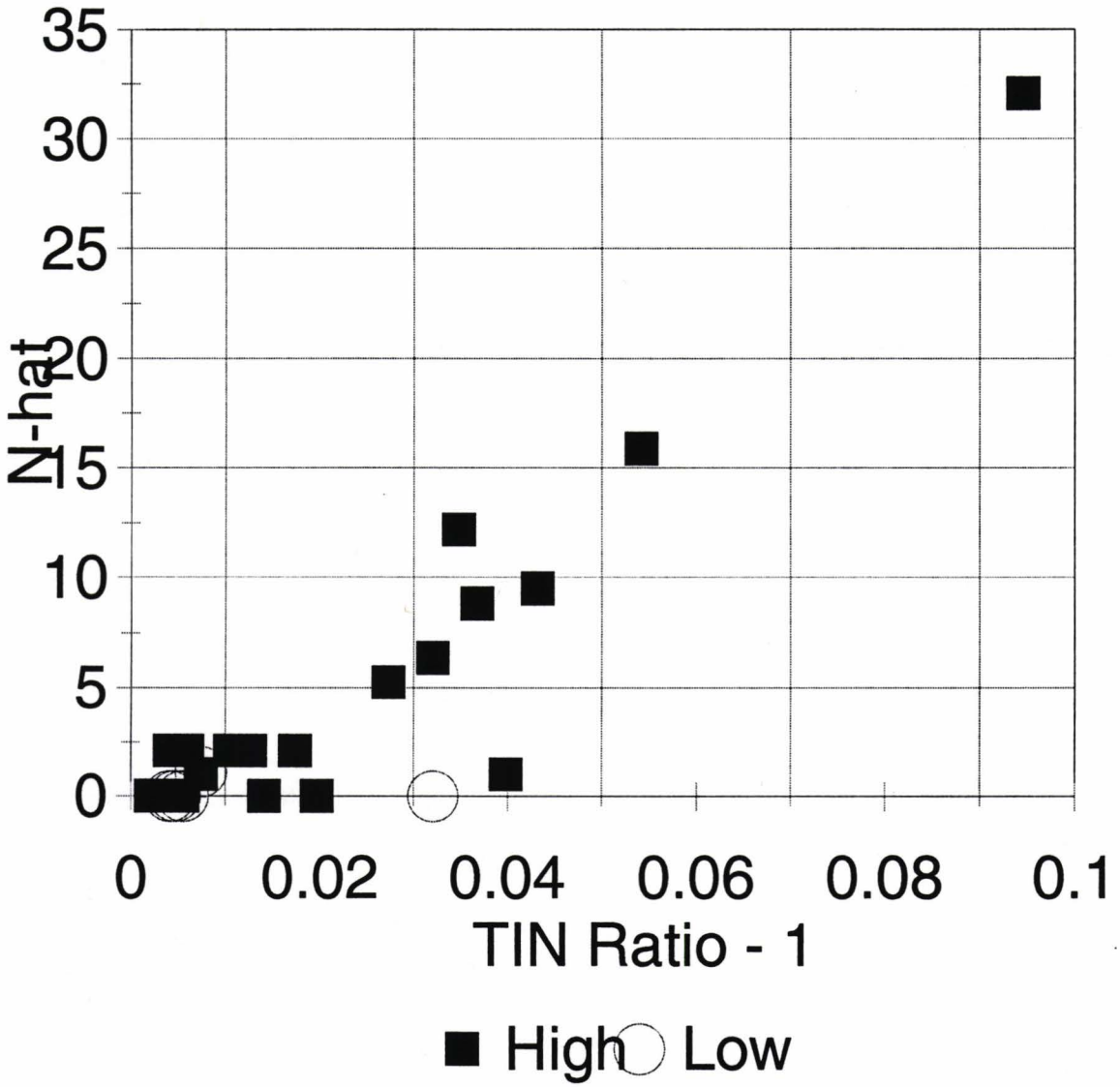

Figure 1. Relationship between $\hat{N}_q$ and TIN Ratio - 1 for the 25 quadrats sampled.

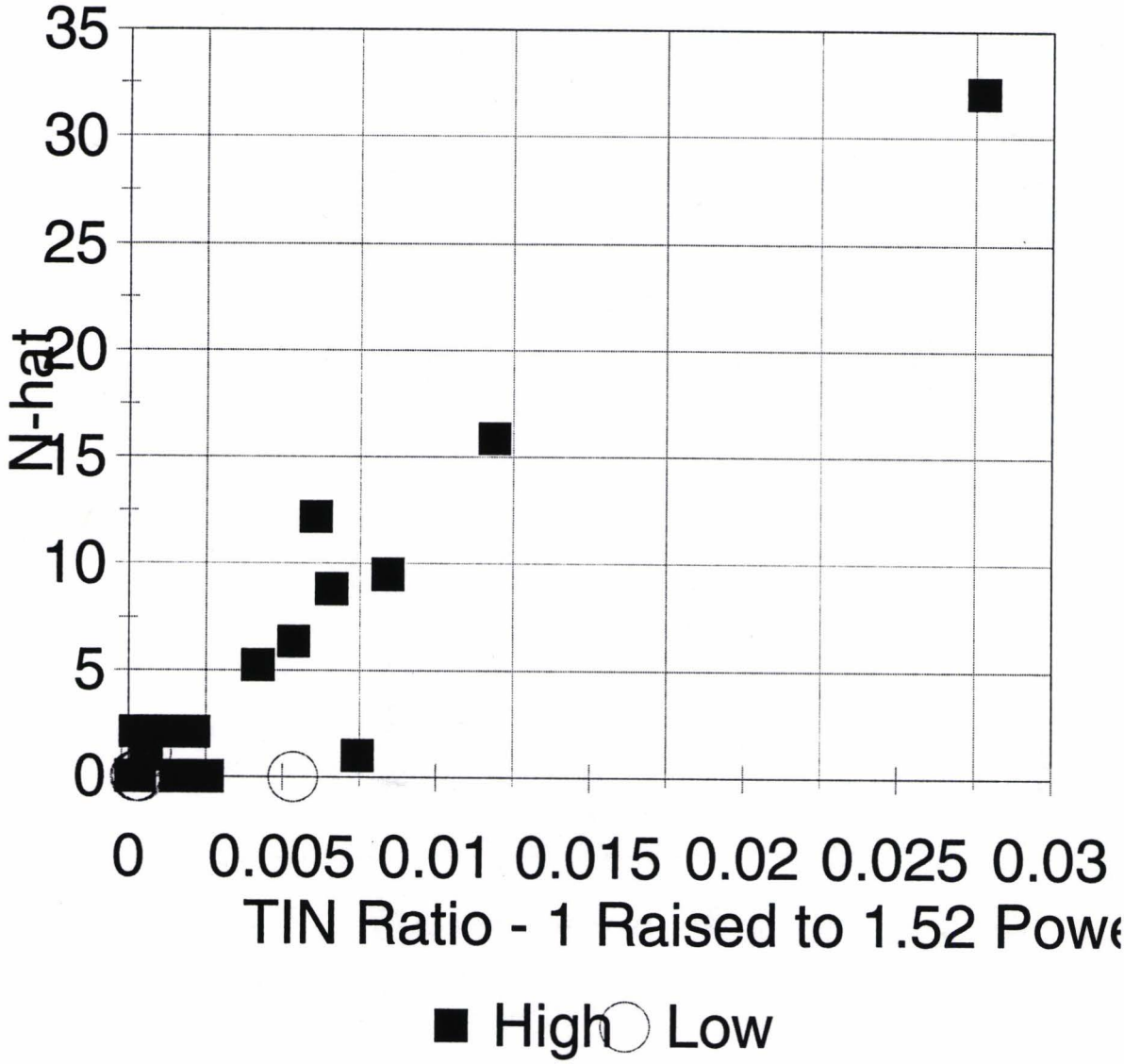

Figure 2. Relationship between $\hat{N}_q$ and TIN Ratio - 1 raised to the 1.52 power for the 25 quadrats sampled.

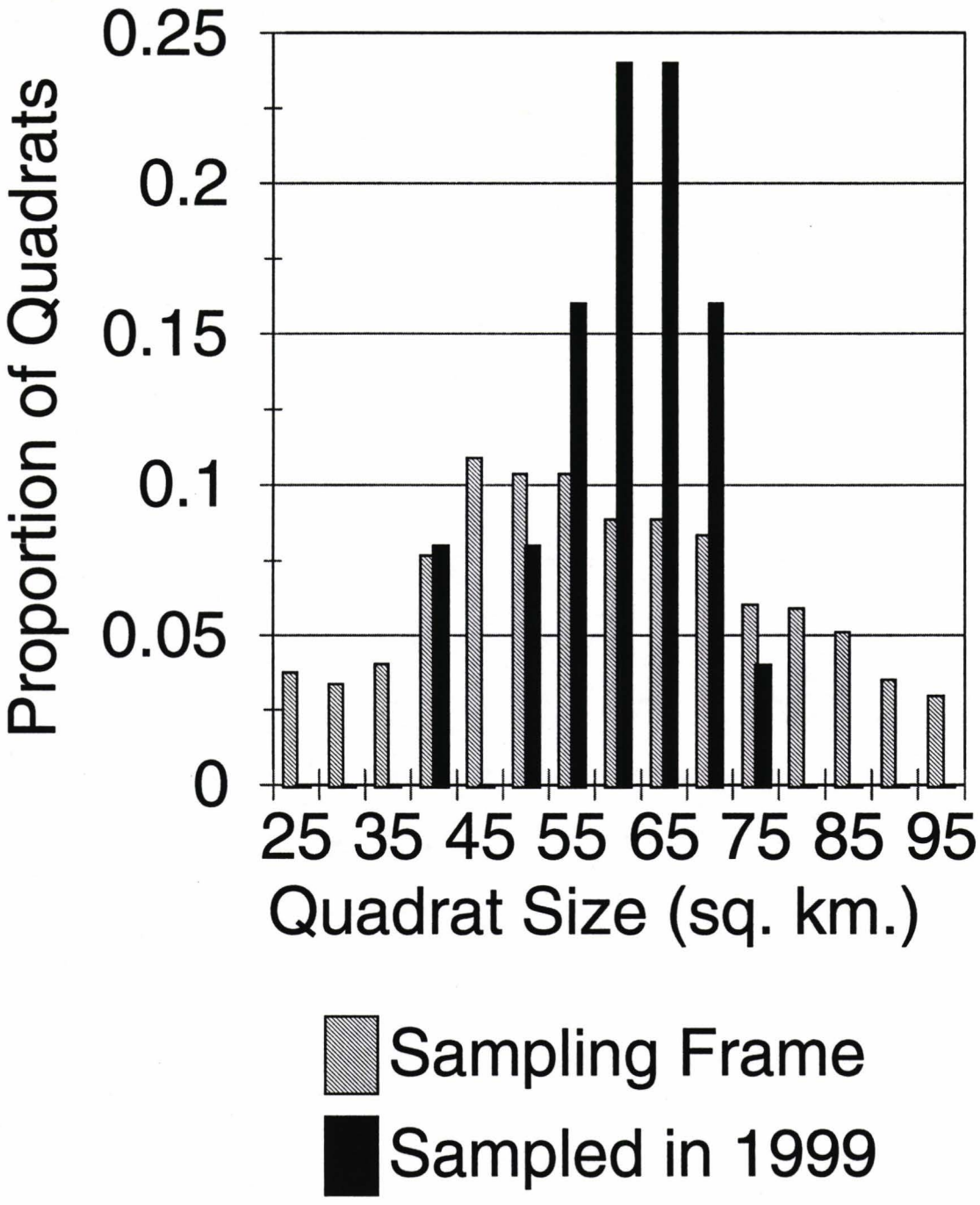

Figure 3. Comparison of quadrat size between sampling frame and quadrats actually sampled in the Mexican Spotted Owl Monitoring Pilot Study conducted in 1999.

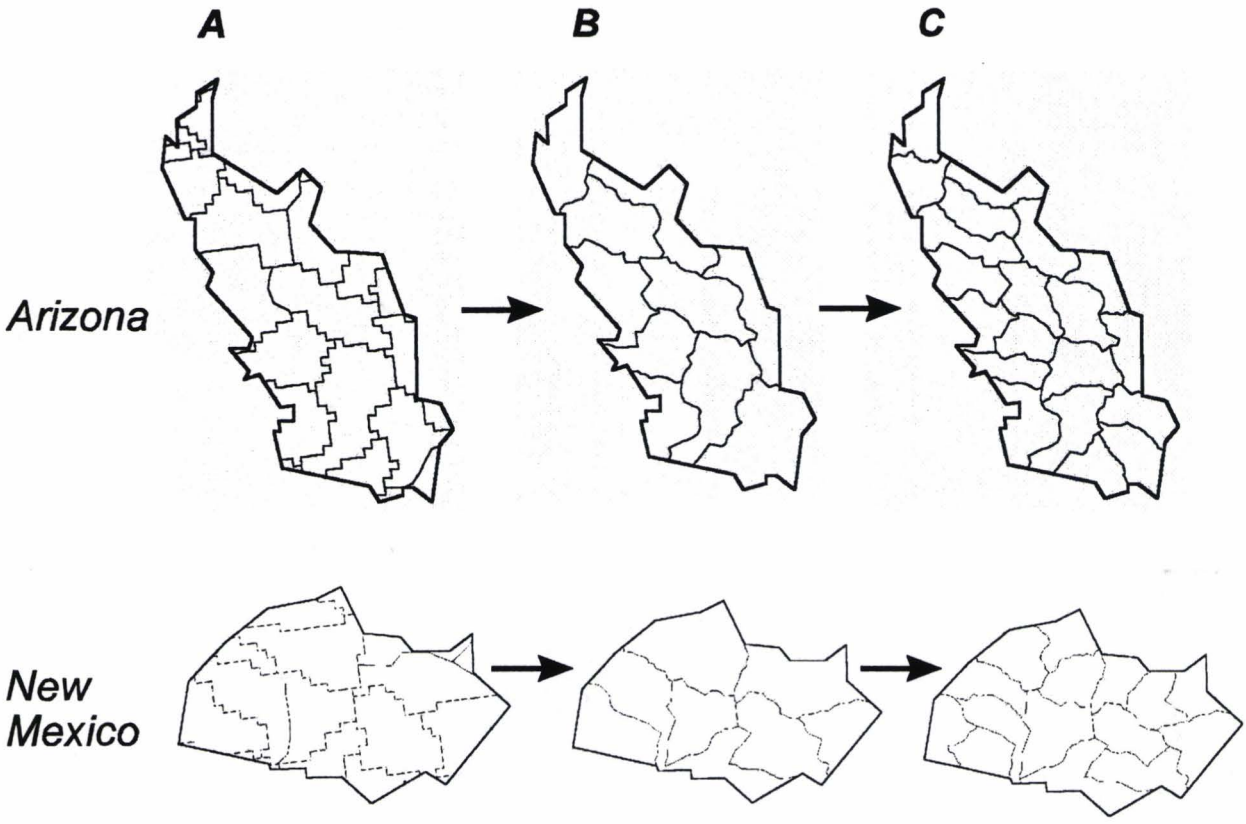

Figure 4. Schematic procedures used to delineate large quadrats (B) from watershed boundaries (A) and small quadrats (C) from large quadrats on the Arizona and New Mexico demographic study areas.

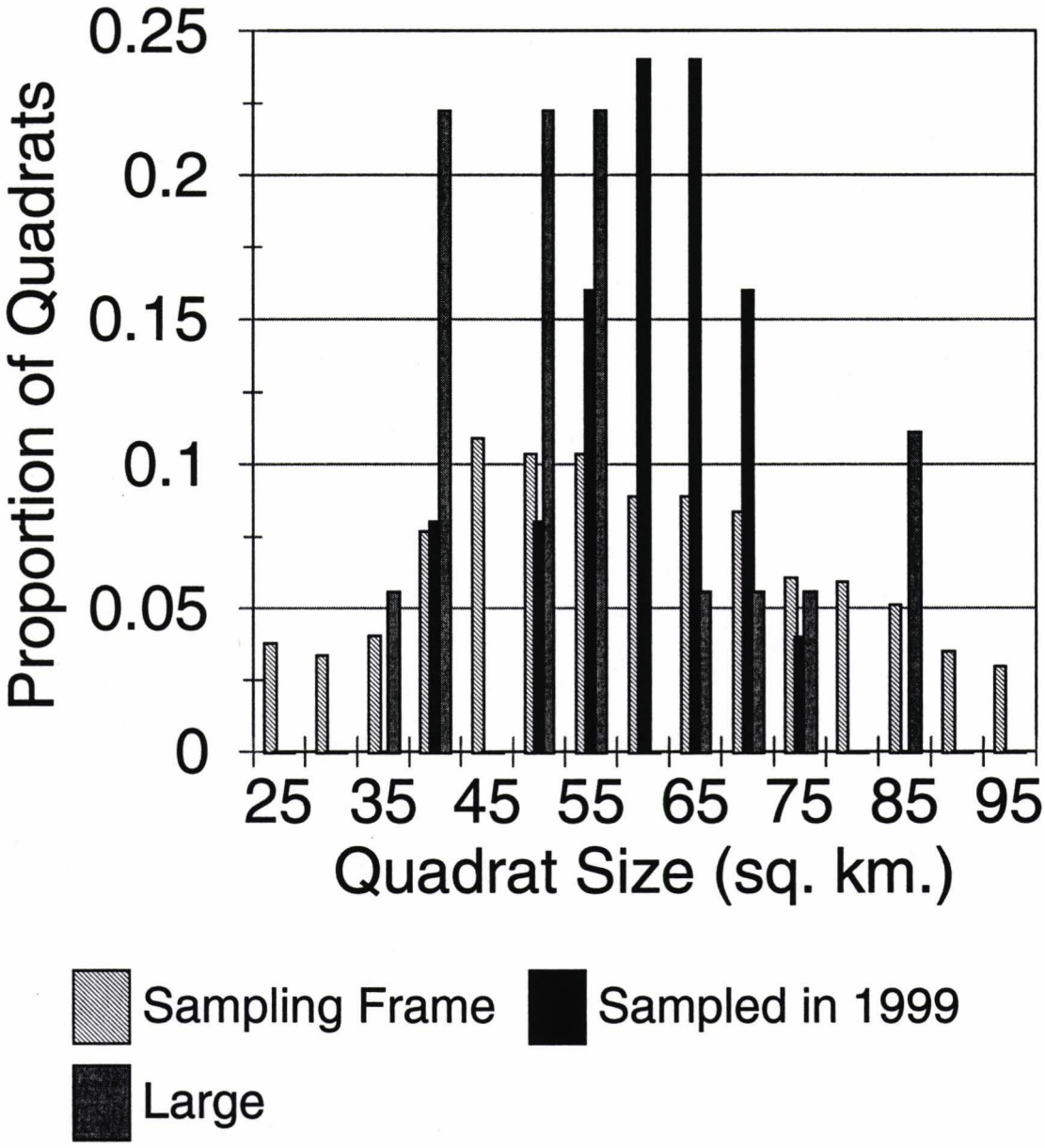

Figure 5. Distribution of large quadrats delineated on demography study areas in relation to quadrats from sampling frame and sampled quadrats used in monitoring pilot study.

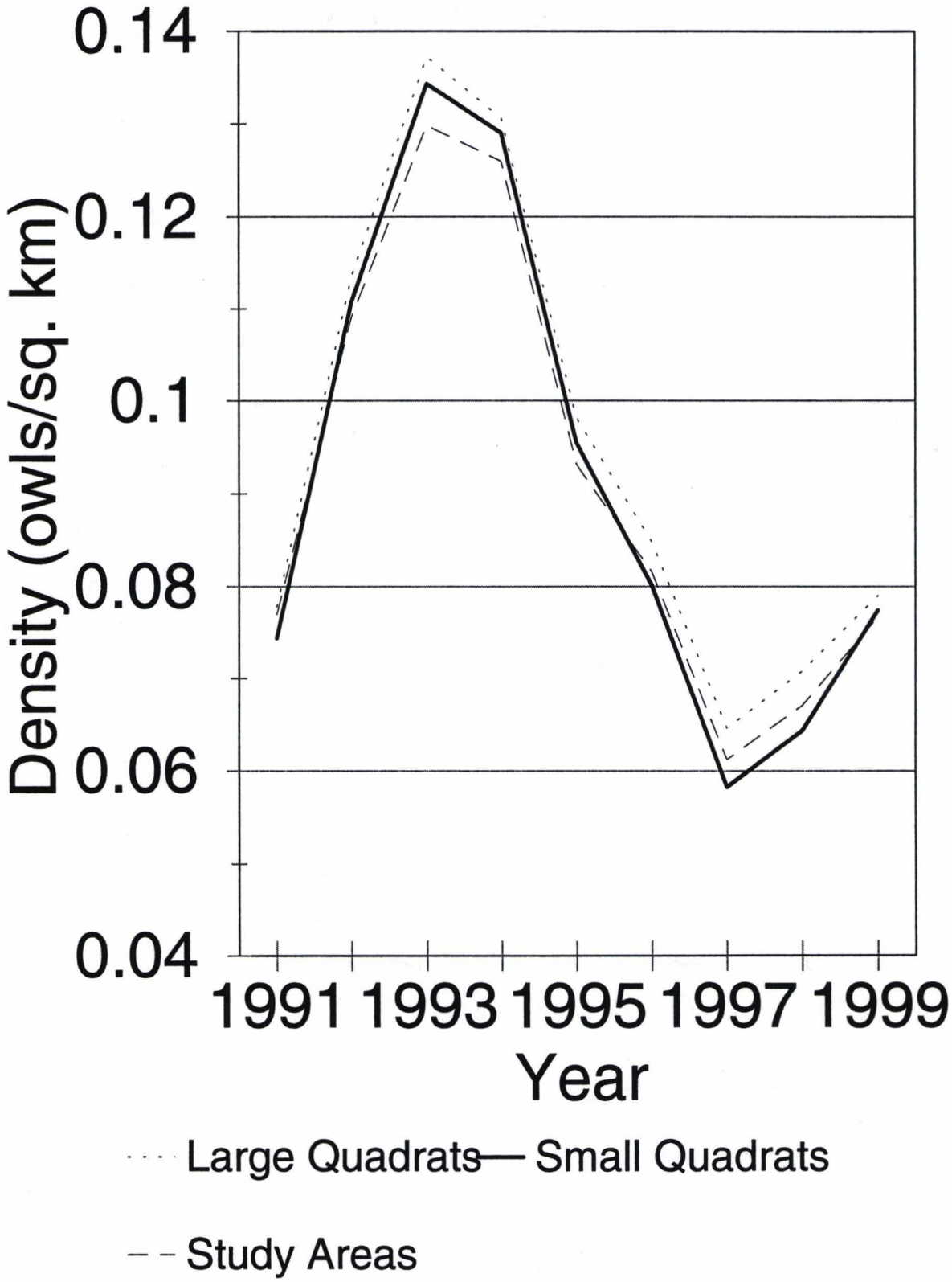

Figure 6. Trends in annual density derived from large and small quadrats delineated on two demography study areas. Annual density estimates averaged over the two study areas are included for comparison.

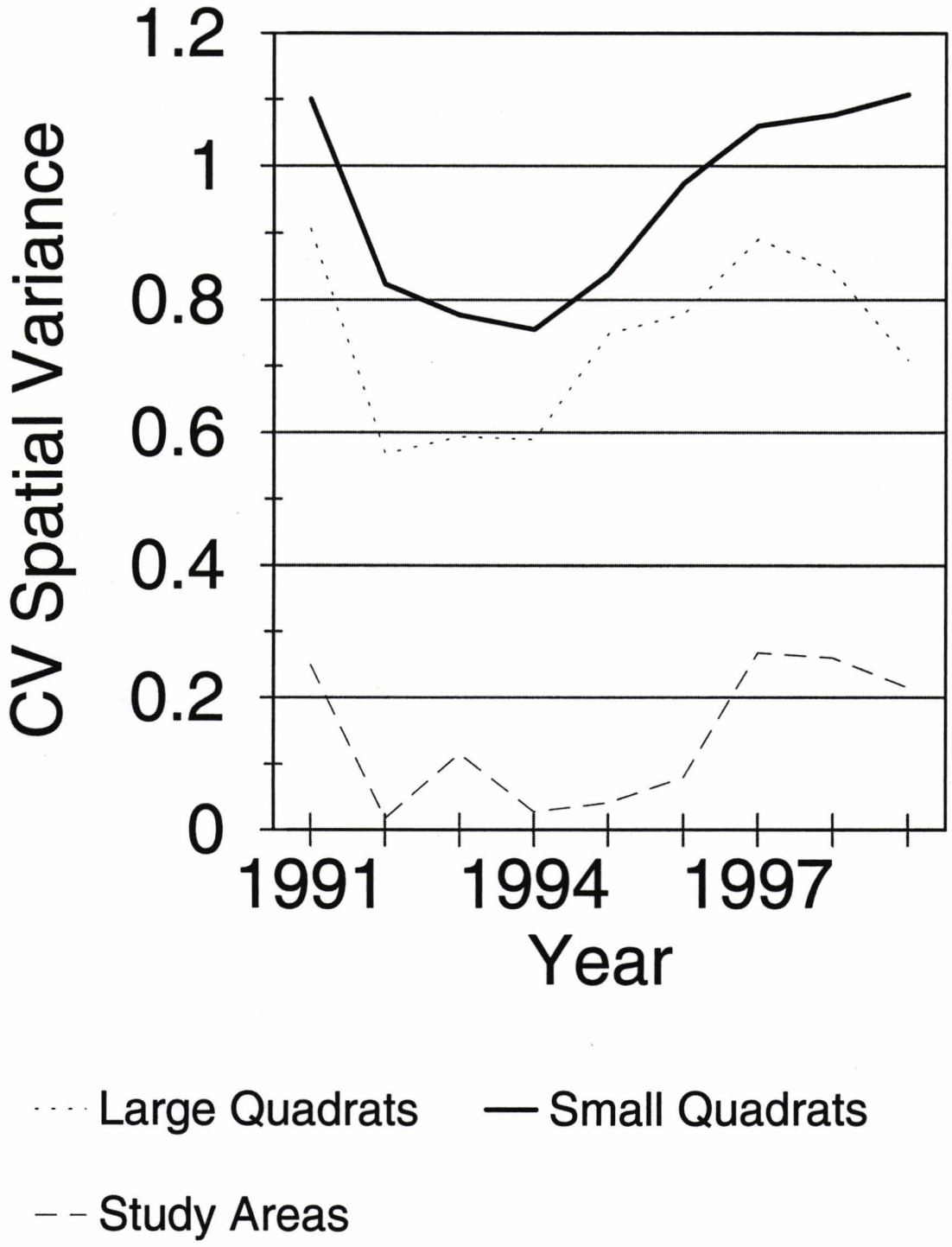

Figure 7. Trends in annual estimates of coefficient of spatial process variation for large and small quadrats derived from demography study areas. Annual density estimates averaged over the two study areas are included for comparison.

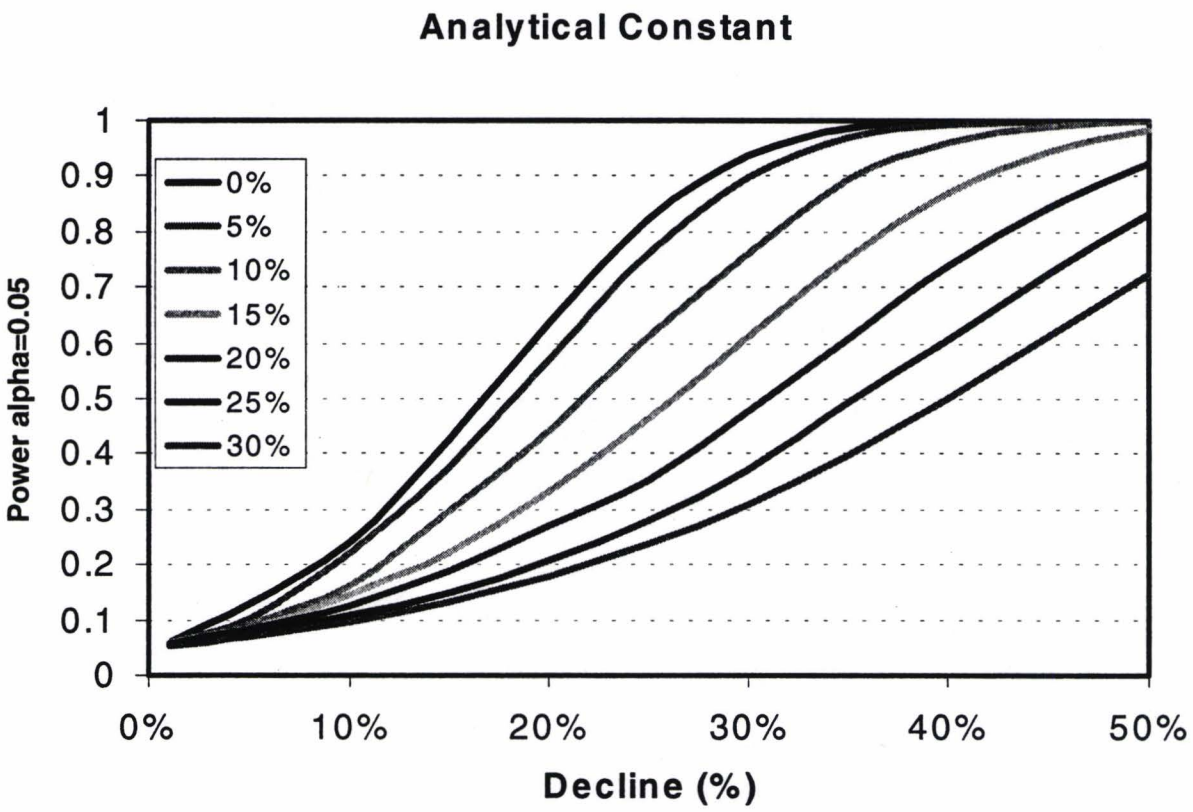

Figure 8. Power curves generated with analytical formulae of Gerrodette (1987) for 7 values of the sampling coefficient of variation and a process standard deviation of 0.1135251. Sampling coefficient of variation was assumed constant and the exponential model of trend was used with 10 years of population estimates.

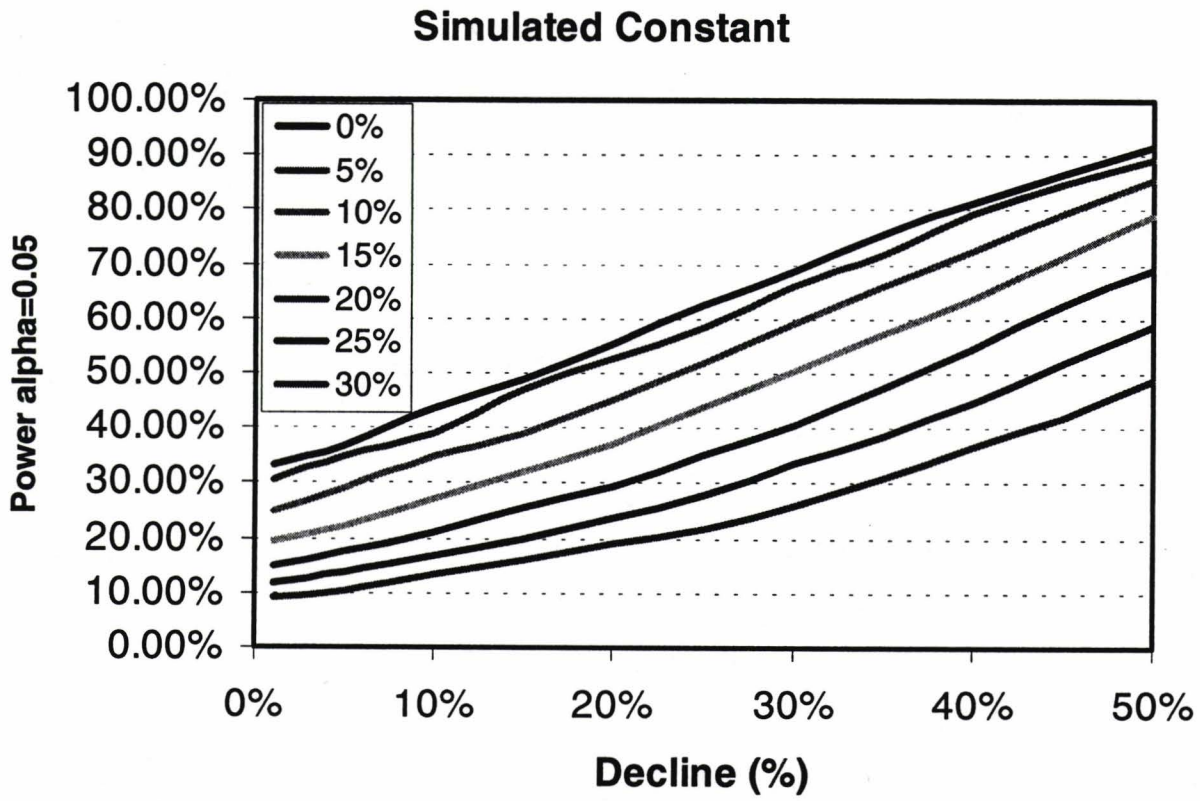

Figure 9. Simulation results for 7 values of the sampling coefficient of variation with a process standard deviation of 0.1135251. An exponential model (Gerrodette 1987) was used to detect trend for 10 years of population estimates.

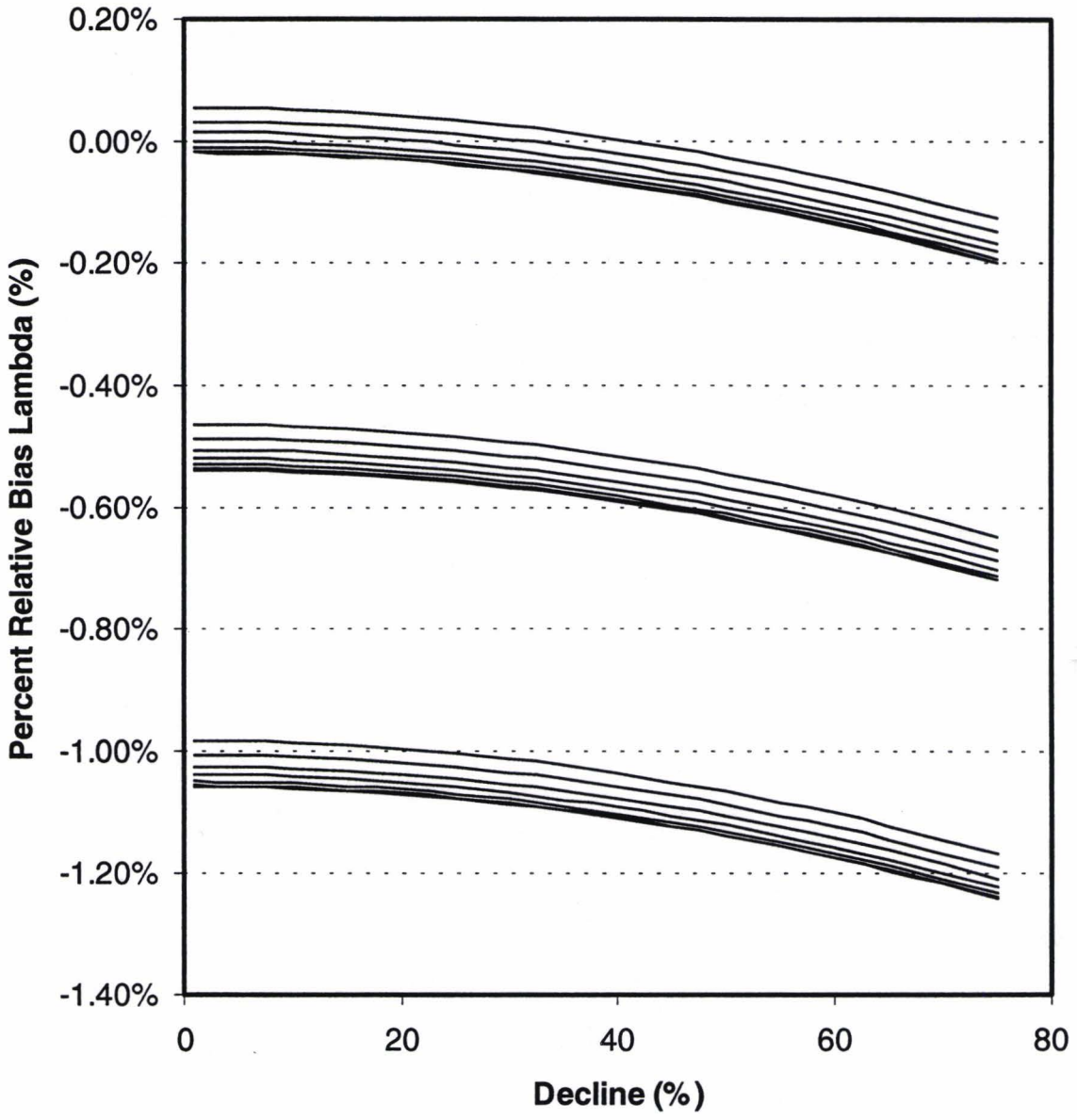

Figure 10. Percent relative bias of estimates of λ for the exponential regression model of trend. The top, middle, and bottom groups of lines are for process standard deviations of lambda of 0.05, 0.10, and 0.15, respectively. Within each group are plotted 7 values of sampling coefficient of 0% (lowest) to 30% (highest) in increments of 5%.

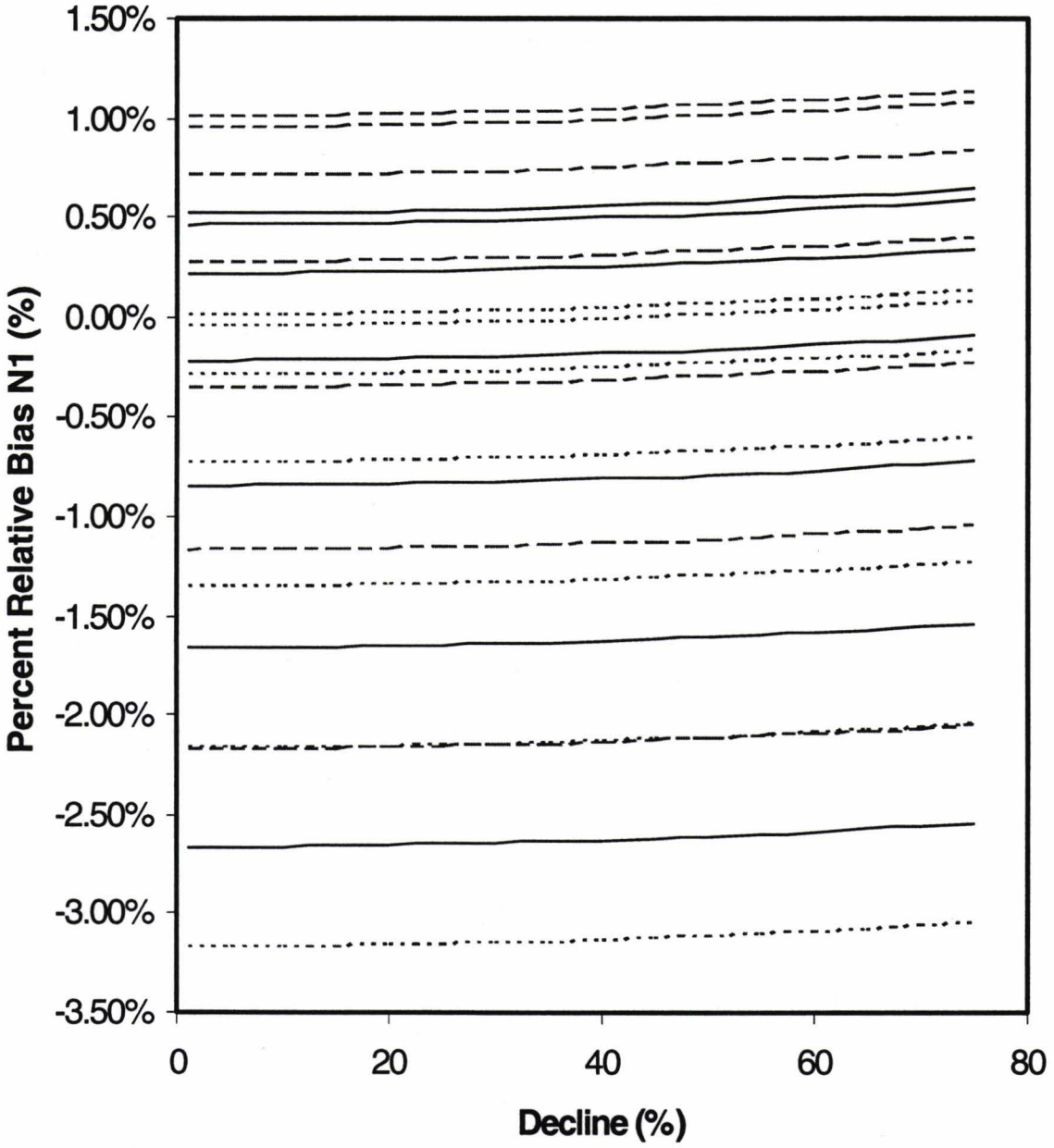

Figure 11. Percent relative bias of estimates of N_1 for the exponential regression model of trend. The short-dashed blue, solid black, and long-dashed red groups of lines are for process standard deviations of lambda of 0.05, 0.10, and 0.15, respectively. Within each group are plotted 7 values of sampling coefficient of 0% (highest) to 30% (lowest) in increments of 5%.

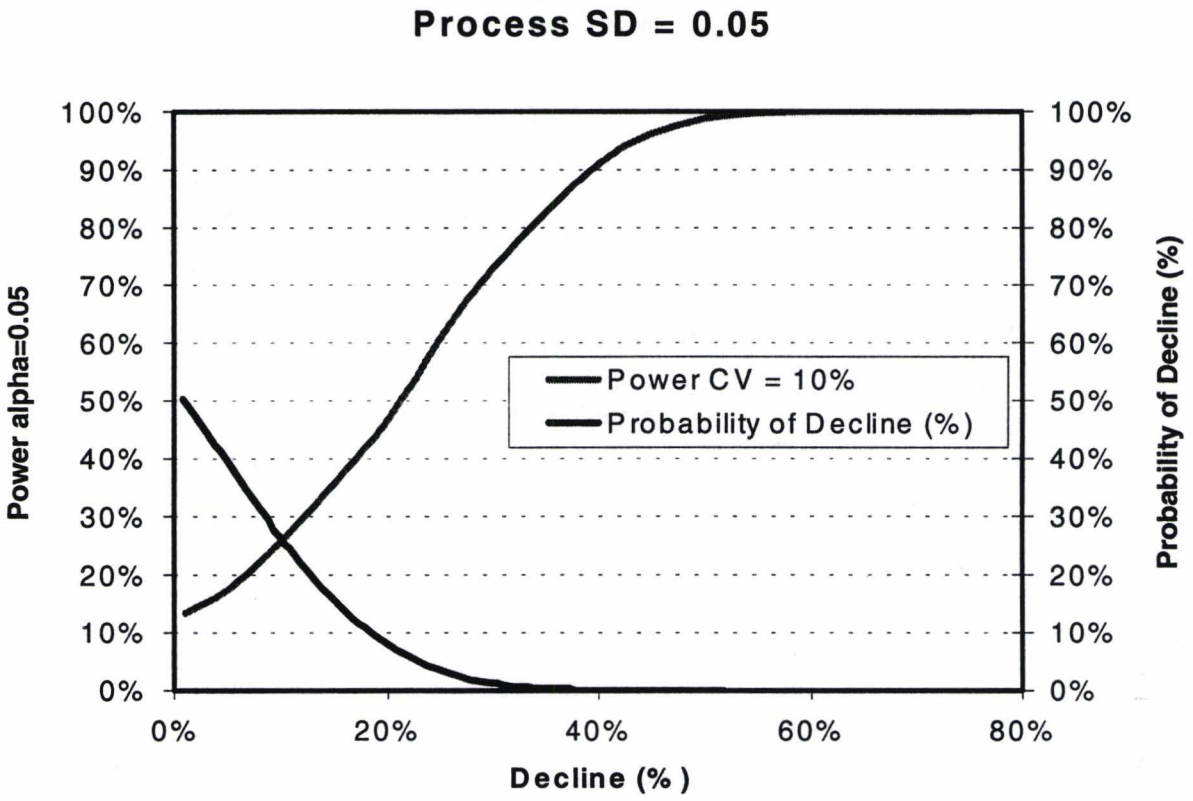

Figure 12. Probability of observing a decline with mean $\lambda = 1$ and process standard deviation equal 0.05 plotted on the same scale as the power to detect a decline with a sampling coefficient of variation of 10%. Power was computed from 10,000 simulations with 10 years of population estimates and the exponential model (Gerrodette 1987).

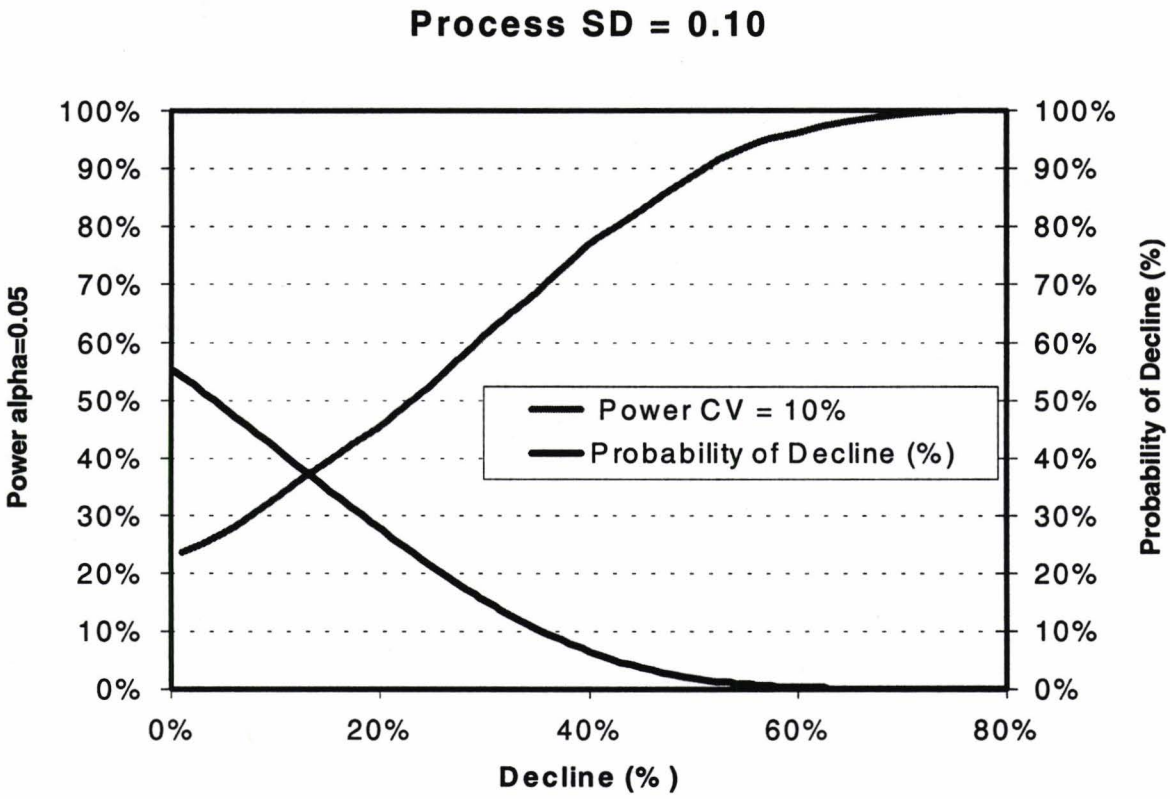

Figure 13. Probability of observing a decline with mean $\lambda = 1$ and process standard deviation equal 0.10 plotted on the same scale as the power to detect a decline with a sampling coefficient of variation of 10%. Power was computed from 10,000 simulations with 10 years of population estimates and the exponential model (Gerrodette 1987).

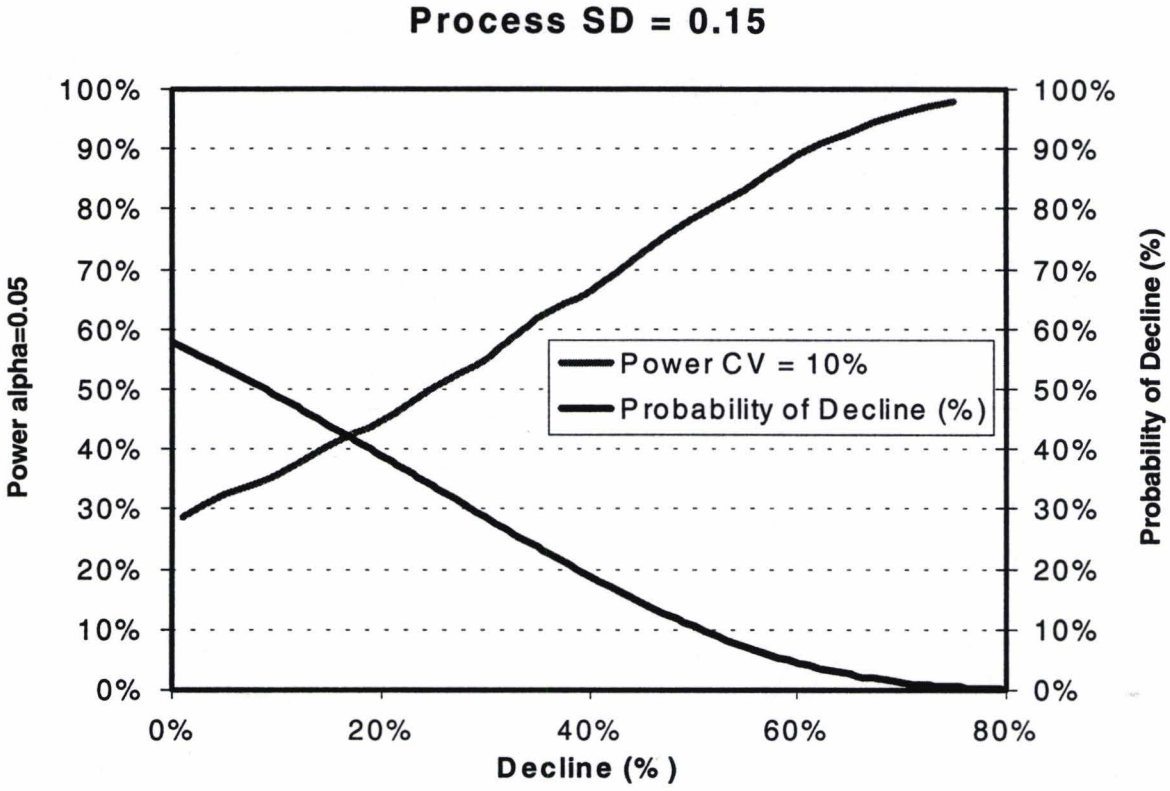

Figure 14. Probability of observing a decline with mean $\lambda = 1$ and process standard deviation equal 0.15 plotted on the same scale as the power to detect a decline with a sampling coefficient of variation of 10%. Power was computed from 10,000 simulations with 10 years of population estimates and the exponential model (Gerrodette 1987).

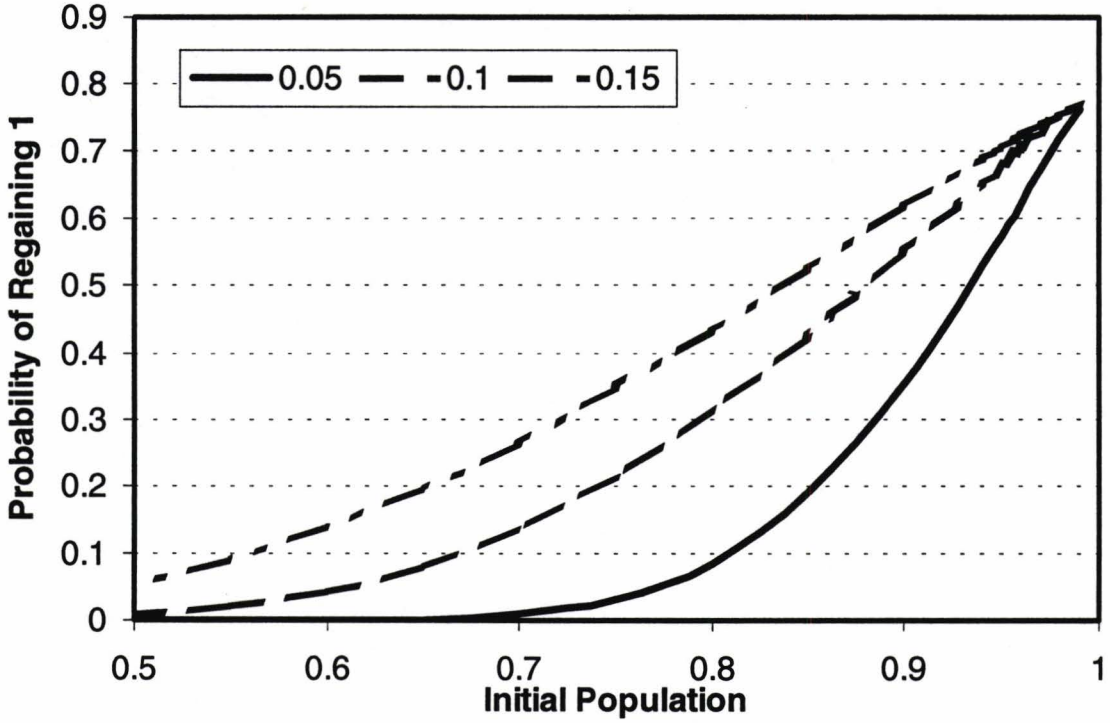

Figure 15. Probability of regaining the mean population size of 1 sometime during the next 10-year period given that the population is currently at some fraction of the mean population size.